DEPARTMENT OF THE INTERIOR
U.S. GEOLOGICAL SURVEY

PREPARED IN COOPERATION WITH THE
STATE OF ALASKA DEPARTMENT OF NATURAL RESOURCES
DIVISION OF MINING AND GEOLOGICAL AND GEOPHYSICAL SURVEYS

GEOPHYSICAL INVESTIGATIONS
MAP GP–992 (SHEET 1 OF 2)

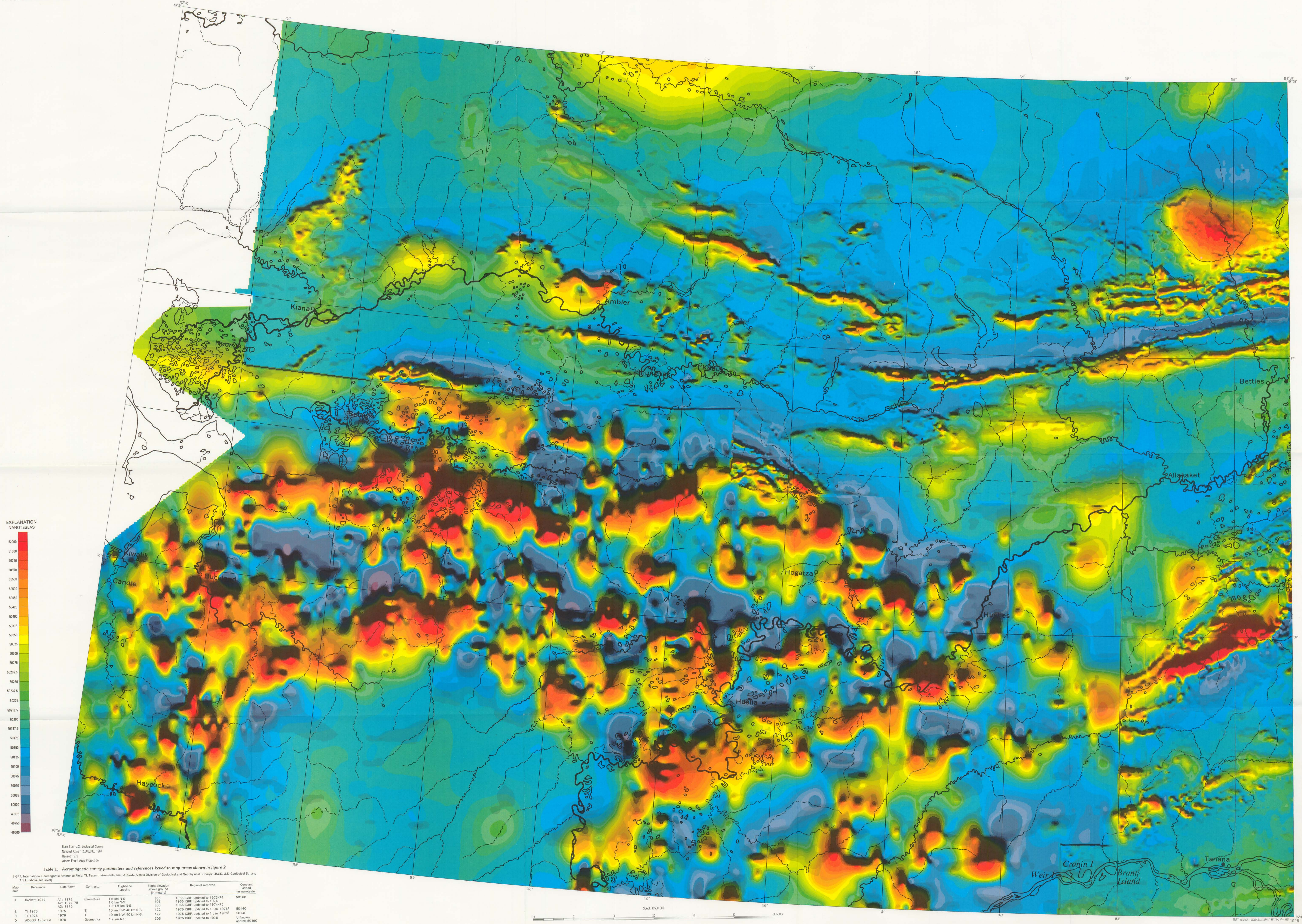

Base from U.S. Geological Survey
National Atlas 1:2,000,000, 1967
Revised 1973
Albers Equal-Area Projection

Table 1. *Aeromagnetic survey parameters and references keyed to map areas shown in figure 2*

[IGRF, International Geomagnetic Reference Field: TI, Texas Instruments, Inc.; ADGGS, Alaska Division of Geological and Geophysical Surveys; USGS, U.S. Geological Survey; A.S.L., above sea level]

Map area	Reference	Date flown	Contractor	Flight-line spacing	Flight elevation above ground (in meters)	Regional removed	Constant added (in nanoteslas)
A	Hackett, 1977	A1: 1973 A2: 1974–75 A3: 1975	Geometrics	1.6 km N-S 1.6 km N-S 1.2-1.6 km N-S	305 305 305	1965 IGRF, updated to 1973–74 1965 IGRF, updated to 1974 1965 IGRF, updated to 1974–75	50160
B	TI, 1975	1975	TI	10 km E-W, 40 km N-S	122	1975 IGRF, updated to 1 Jan, 1976[1]	50140
C	TI, 1975	1976	TI	10 km E-W, 40 km N-S	122	1975 IGRF, updated to 1 Jan, 1976[1]	50140
D	ADGGS, 1982 a-d	1978	Geometrics	1.2 km N-S	305	1975 IGRF, updated to 1978	Unknown, approx. 50190
E	USGS, 1973 a-g	1972	Aero Service	2 km N-S	305	1965 IGRF, updated to 1972	0
F	USGS, 1974 a-d	1973	Geometrics	1.6 km N-S	305	1965 IGRF, updated to 1973	Unknown, approx. 50220
G	Brosgé and others, 1970	1965	USGS	Variable, ~16 km	1524 A.S.L.	Unknown regional removed	49950
H	TI, 1976	1976	TI	10 km E-W, 40 km N-S	122	1975 IGRF, updated to 1976	50185
I	TI, 1978	1977	TI	10 km E-W, 40 km N-S	122	1975 IGRF, updated to 1976	50185

[1] IGRF – Due to apparent errors in IGRF removal in area C by the contractor, areas B and C were difficult to merge. In order to facilitate merger, the IGRF of 1 January, 1976, about midway between the survey dates, was removed from the raw Earth's magnetic field in areas B and C.

MAGNETIC SURVEYS AND DATA REDUCTION

This is a map of the total intensity of the Earth's magnetic field corrected for the slope of the International Geomagnetic Reference Field (IGRF). In addition, a tilted-planar regional has been removed to approximately correct for errors in the 1965–1975 IGRF. It is a digital map compiled from 8 different surveys. Figure 1 shows the boundary of the map area superimposed on an index map of 1:250,000-scale quadrangles. Locations of the individual survey areas are shown in figure 2. Specifications for the surveys are given in table 1.

A comparison of the flight-line tracks shown in figure 2 with the aeromagnetic map shows that many of the changes in magnetic texture reflect flight-line spacing. Areas A, D, E, and F all used magnetic tapes of digital data collected along north-south flight lines between 1.2 and 2 km apart, flown nominally 305 m above terrain. Flight-line tracks are not available digitally for area A, which was digitized from 1:63,360-scale contour maps. Area G has the worst coverage—the data were digitized by hand along flight lines on a 1:1,000,000-scale hand-contoured map. Data for areas B, C, H, and I were obtained digitally along flight lines spaced 10 km apart east-west and 40 km apart north-south, 122 m above the terrain.

Data along flight lines (or in area A, along contour lines) were gridded using minimum-curvature algorithm MINC (Webring, 1981). A grid interval of 0.4064 km, or from 1/3 to 1/5 of the flight-line spacing, was used for areas A, D, E, and F. In areas B, C, G, H, and I, a wider grid interval of 2.032 km, or about 1/5 the flight-line spacing, was used. These coarser grids were spline-interpolated to 0.4064 km, the grid interval required to make 1:500,000-scale plots on the Applicon color plotter, for editing and interpretation.

The final aeromagnetic map was printed from four color-separation negatives produced on the Scitex computer system. Contour levels are shown by a nonlinear color scale that has a contour interval of 12.5 nT in the middle of the range (where most of the low-gradient field areas are) and larger contour intervals at the bottom and top of the range. Superimposed on the color contours are dark and light patterns of shaded relief simulating illumination of a three-dimensional model of the magnetic field by a light source 40 degrees above the southern horizon (M. Webring, unpub. computer documentation for program CSRELIEF, 1987). Program CSRELIEF was used to produce three color grid files and one gray-shade grid file at an interval of 0.4064 km. These grids were then regridded to 0.25 km and converted to the Scitex format to create the color-separation negatives. The shaded-relief map better delineates short-wavelength, low-amplitude variations in the magnetic field, and is easier for many users to interpret geologically, than black-and-white or color-slice contour maps.

The spotted pattern of highs and lows in areas B, C, G, H, and I is in part an artifact of machine contouring of widely-spaced flight-line data. Short-wavelength linear trends may be present that cannot be resolved by the available data. For example, the westernmost part of area D (lat. 66° 30′–66°45′ N., long. 156°–156°30′ W.) has short-wavelength, linear anomalies not apparent in the coarser data of area B.

A north-south grain is visible in areas of low magnetic intensity in areas D, E, and F. This grain is probably an artifact of imperfect removal of magnetic diurnal variations in adjacent flight lines.

The IGRF had been removed from flight-line data by previous authors in areas A, D, E, F, H, and I (see table 1 for details). An unknown regional field had been removed from the contour map of area G. In area C, the IGRF removal appeared to be erroneous; so in order to merge data in areas B and C, the IGRF was calculated for a time approximately midway between the survey dates and removed from both data sets (table 1).

The datum levels of the various surveys were different. By comparing surveys at their boundaries, constants were determined (table 1) that were added to data from individual surveys before merging. An examination of the color-shaded relief map shows that the datum match is imperfect. Color breaks occur at nearly all boundaries between surveys, partly because datum levels do not match and partly because of changes of data density. No attempt was made to continue upward the widely spaced data flown at 122 m above terrain to make it match the closely spaced data flown 305 m above terrain. Upward continuation is a low-pass filter, and low-pass filtering could not be avoided when gridding the 122 m data at an interval of 2.032 km.

Most of the mismatch between surveys cannot be explained by a datum error. For example, area B plus C is 50 to 100 nT higher than area A in the northwest, but 50 to 100 nT lower than area E in the southeast. There appears to be a tilt, as well as a datum shift. The problem may be caused in part by inconsistent IGRF removal by different contractors. In retrospect, a better map might have been made by starting with raw total field data if available on magnetic tape; adding back in the appropriate IGRF to data that were hand digitized or for which raw total field data were unavailable; and then subtracting the appropriate Definitive Geomagnetic Reference Field (Peddie, 1983).

In the datum-shifted data, a regional positive gradient of nearly 400 nT occurs from northwest to southeast (fig. 3). This can be explained by errors in the 1965 through 1975 IGRF. Peddie (1983, fig. 3) shows that the 1975 IGRF was 300 nT too low near the Alaska-Canada border, and 100 nT too high near the Bering Strait. On the color-shaded relief map, the slope of the least-squares fit plane shown in figure 3 has been removed, producing a map that approximates the Earth's total magnetic field minus the slope of the Definitive Geomagnetic Reference Field (Peddie, 1983). The approximate total intensity of the field is retained for those who need it to calculate induced magnetization in anomaly sources.

The aeromagnetic data from which the map was produced, gridded at a interval of 0.4064 km, are available from the National Geophysical Data Center, 325 Broadway, Boulder, Colorado 80303.

INTERPRETATION OF MAGNETIC DATA

No detailed interpretation of the aeromagnetic map is given here, but the following general interpretation will help to orient the reader to the map. A small-scale, aeromagnetic, color-shaded relief map annotated with geologic and geographic names (fig. 4) is provided to help the reader identify features described in the text. Further information can be found in the following publications. Interpretations of individual quadrangles are available for Chandalar (Cady, 1979), Ambler River (Hackett, 1980), Survey Pass (Cady and Hackett, 1982), and Circle (Cady and Weber, 1983). Broad regional interpretations were published by Brosgé and others (1970), Cady (1986), and Cady (1987). A detailed interpretation of the area west of long. 150° W., is available in Cady (1989). Geology of the western two-thirds of the area is available in Patton and others (in press).

In the southwestern part of the map, as far east as long. 153°30′ W., a large horseshoe-shaped pattern of magnetic highs about 400 km in diameter is caused by mafic and intermediate extrusive rocks of the informally designated Cretaceous Koyukuk magmatic arc (fig. 4). Magnetic lows within this belt are commonly caused by granitoid plutons. The horseshoe-shaped hole is caused by a thick section of nonmagnetic Cretaceous marine and nonmarine sedimentary rocks.

An intense northeast-trending magnetic high in the Tanana and Bettles quadrangles is caused by ultramafic rocks and layered gabbros of the northwest-dipping, informally designated Jurassic(?) Kanuti ophiolite (Cady, 1986). To the northeast, in the Jim River area, a similar intense magnetic high is caused by Cretaceous granitoid plutons that appear to have become magnetic because of contamination by ophiolitic material. The magnetic high may also be caused by ultramafic rocks and layered gabbro hidden beneath a cover of metavolcanic rocks. Southeast of the Kanuti ophiolite are magnetic lows caused by nonmagnetic Cretaceous plutons of the Ruby geanticline.

Prominent areas of low magnetic intensity and low magnetic relief in the Brooks Range are caused by thick sections of nonmagnetic Precambrian and Paleozoic meta-sedimentary rocks and, in the Survey Pass and western Wiseman quadrangles, by large nonmagnetic Devonian plutons. Subtle magnetic highs commonly occur over contact aureoles at the margins of these plutons. Between long. 148° W. and long. 160° W., the south boundary of the Brooks Range is marked by a magnetic low coincident with nonmagnetic Paleozoic phyllite and metagraywacke associated with the Angayucham thrust (Dillon, 1989). North of the magnetic low are short-wavelength, elongate magnetic highs generally caused by magnetic schists of Paleozoic and Precambrian(?) age. A few of these highs are labeled P̶zp€s in figure 4. In the Chandalar and eastern Wiseman quadrangles, magnetic highs commonly coincide with contact metamorphic aureoles in schist surrounding cores of small, nonmagnetic, granitoid bodies.

Immediately south of the Angayucham thrust, east-west linear magnetic highs are caused by mafic volcanic rocks and rare associated ultramafic rocks of the Devonian through Jurassic Angayucham terrane (ANG in fig. 4). The magnetic highs over the Angayucham terrane are much smaller than the magnetic highs over the Kanuti ophiolite, suggesting that magnetic ultramafic rocks and layered gabbros are much less abundant in the Angayucham terrane than in the Kanuti ophiolite. Within the V, open to the southwest, formed by the Angayucham terrane and Kanuti ophiolite there are subdued highs caused by buried sources and lows caused by thick accumulations of Cretaceous marine sedimentary rocks.

The Yukon-Tanana terrane in the Circle quadrangle and the southeastern Livengood quadrangle contains northeast-trending, low-amplitude, short-wavelength, magnetic highs inferred to be caused by Precambrian(?) and Paleozoic magnetic chloritic schist. Some of these highs are labeled P̶zp€s in figure 4. Magnetic lows are caused by nonmagnetic Cretaceous to Tertiary granitoid bodies that commonly occur in the cores of antiforms. These anomalies are bounded to the north by the Tintina fault zone, which is marked by a discontinuous belt of magnetic highs. In the central Livengood quadrangle and the southern Tanana quadrangle, a discontinuous belt of magnetic anomalies caused by Cambrian(?) ultramafic rocks probably marks a southwest-trending splay of the Tintina fault zone.

North of the Tintina fault zone, between long. 144° W. and long. 153° W., is a discontinuous belt of short-wavelength magnetic highs (labeled T̶Mr in fig. 4) caused by magnetic layered gabbros and minor ultramafic rocks of the Mississippian to Triassic(?) Rampart Group. A prominent magnetic anomaly in the southern Beaver quadrangle is caused by a shallow buried source, probably belonging to the Rampart Group. The rest of the Beaver quadrangle contains many magnetic anomalies caused by mafic intrusive and extrusive rocks and granitoid plutons that have not been studied in detail.

Magnetic highs over exposed and inferred buried granitoid plutons (gr in fig. 4) occur in the Wiseman and Chandalar quadrangles and in the Tintina fault zone and related faults in the Circle, Livengood, and Tanana quadrangles. An intense magnetic anomaly (labeled gr) in the Melozitna quadrangle coincides with magnetic quartz monzonite.

In the eastern part of the map (areas G, H, and I in fig. 2), the data quality is very low. An interpretation of a reconnaissance aeromagnetic survey (reproduced in part in area G) was made for the eastern areas by Brosgé and others (1970). Some of the most prominent magnetic anomalies in the area occur over the Christian mafic and ultramafic body (Patton and others, 1977), which is part of the Rampart Group, in the central Christian and western Coleen quadrangles. A buried source is inferred for a magnetic high in the southeastern corner of the Charley River quadrangle, just north of the Tintina fault zone. The source could be a nonmagnetic granitoid pluton similar to those inferred in the Tintina fault zone of the eastern Circle quadrangle. An alternative explanation for the magnetic highs over the Tintina fault zone is metamorphosed flysch (W. D. Stanley, oral commun., 1986).

The data of poor quality in areas G, H, and I do not lend themselves to detailed interpretation. One can only guess as to the nature of the magnetic basement of Yukon Flats, although it may belong to the Rampart Group, which is exposed both to the north and south. The coarse data reveal very little about the structure of the Christian mafic and ultramafic body. In areas B and C, the data quality is equally poor, but because of the giant scale of the Koyukuk magmatic arc, the anomalies form a more coherent pattern. The fine detail visible where the westernmost extension of area D overlaps the Koyukuk magmatic arc shows that better aeromagnetic data would help to resolve the fine structure of the arc.

ACKNOWLEDGEMENTS

Esther Sandoval digitized analog aeromagnetic maps in areas A and G. Robert L. Fargo, Michael G. Medberry, and Timothy L. Nowfel helped with portions of the data processing. Computer programs written by Michael W. Webring, Richard H. Godson, Richard W. Saltus, and Ronald E. Sweeney made the map compilation possible.

REFERENCES CITED

Alaska Division of Geological and Geophysical Surveys, 1982a, Aeromagnetic map of the Wiseman quadrangle, Alaska: Alaska Open-File Report 176, scale 1:250,000.

_______1982b, Aeromagnetic map of the northern portion of the Shungnak quadrangle, Alaska: Alaska Open-File Report 177, scale 1:250,000.

_______1982c, Aeromagnetic map of the northern half of the Hughes quadrangle, Alaska: Alaska Open-File Report 178, scale 1:250,000.

_______1982d, Aeromagnetic map of the Bettles quadrangle, Alaska: Alaska Open-File Report 179, scale 1:250,000.

Brosgé, W.P., Brabb, E.E., and King, E.R., 1970, Geologic interpretation of reconnaissance aeromagnetic survey of northeastern Alaska: U.S. Geological Survey Bulletin 1271–F, p. F1–F14.

Cady, J.W., 1979, Aeromagnetic map and interpretation of the Chandalar quadrangle, Alaska: U.S. Geological Survey Miscellaneous Field Studies Map MF–878C, scale 1:250,000.

_______1986, Geophysics of the Yukon-Koyukuk province: U.S. Geological Survey Circular 978, p. 21–25.

_______1987, Preliminary geophysical interpretation of the oceanic terranes of interior Alaska– Evidence of thick crust of intermediate density, *in* Scheibner, E., and Leitch, D. C., eds., Terrane accretion and orogenic belts: American Geophysical Union Geodynamic Series, v. 9, p. 301–305.

_______1989, Geologic implications of topographic, gravity, and aeromagnetic data in the northern Yukon-Koyukuk province and its borderlands, Alaska: Journal of Geophysical Research, v. 94, p. 15821–15841.

Cady, J.W., and Hackett, S.W., 1982, Aeromagnetic map and interpretation, Survey Pass quadrangle, Alaska: U.S. Geological Survey Miscellaneous Field Studies Map MF–1176G, scale 1:250,000.

Cady, J.W., and Weber, F.R., 1983, Aeromagnetic map and intepretation of magnetic and gravity data, Circle quadrangle, Alaska: U.S. Geological Survey Open-File Report 83–170–C, scale 1:250,000.

Dillon, J.T., 1989, Structure and stratigraphy of southern Brooks Range and northern Koyukuk basin near the Dalton Highway, *in* C. G. Mull and K. E. Adams, eds., Dalton Highway, Yukon River to Prudhoe Bay, Alaska—bedrock geology of the eastern Koyukuk basin, central Brooks Range, and east-central Arctic slope: Alaska Division of Geological and Geophysical Surveys Guidebook 7, v. 2, p. 157–187.

Hackett, S.W., 1977, revised 1980, Aeromagnetic map of southwestern Brooks Range: Alaska Division of Geological and Geophysical Surveys Geologic Report 56, scale 1:250,000.

_______1980, Aeromagnetic interpretation maps of the Ambler River quadrangle, Alaska: U.S. Geological Survey Open-File Report 78–120K, scale 1:250,000.

Patton, W.W., Jr., Tailleur, I.L., Brosgé, W.P., and Lamphere, M.A., 1977, Preliminary report on the ophiolites of northern and western Alaska, *in* Coleman, R.G., ed., North American ophiolites: Oregon Department of Geology and Mineral Industries Bulletin 95, p. 51–57.

Patton, W.W., Box, S.E., Moll-Stalcup, D.J., and Miller, T.P., in press, Geology of west-central Alaska, *in* Plafker, G., Jones, D.L., and Berg, H.C., eds., Geology of Alaska: Boulder, Colo., Geological Society of America, The Geology of North America.

Peddie, N.W., 1983, International geomagnetic reference field—its evolution and the difference in total field intensity between new and old models for 1965–1980: Geophysics, v. 48, no. 12, p. 1691–1696.

Texas Instruments, Inc., 1975, Airborne geophysical survey, Copper River and Seward-Selawik areas, Alaska: available from U.S. Department of Energy, Grand Junction, Colo., report GJO–1653.

_______1976, Aerial gamma-ray and magnetic survey of the Bethel and Yukon areas, Alaska: available from U.S. Department of Energy, Grand Junction, Colo., report GJBX–5(77).

_______1978, Aerial radiometric and magnetic reconnaissance survey of the Eagle-Dillingham area, Alaska: available from U.S. Department of Energy, Grand Junction, Colo., report GJBX–113(78).

U.S. Geological Survey, 1973a, Aeromagnetic survey, eastern part of the Bettles quadrangle, northeast Alaska: U.S. Geological Survey Open-File Report 73–305, scale 1:250,000.

_______1973b, Aeromagnetic survey, eastern part of the Wiseman quadrangle, northeast Alaska: U.S. Geological Survey Open-File Report 73–306, scale 1:250,000.

_______1973c, Aeromagnetic survey, Melozitna A–1 quadrangle, northeast Alaska: U.S. Geological Survey Open-File Report 73–307, scale 1:63,360.

_______1973d, Aeromagnetic survey, Tanana quadrangle, northeast Alaska: U.S. Geological Survey Open-File Report 73–308, scale 1:250,000.

_______1973e, Aeromagnetic survey, western half of the Beaver quadrangle, northeast Alaska: U.S. Geological Survey Open-File Report 73–309, scale 1:250,000.

_______1973f, Aeromagnetic survey, western half of the Chandalar quadrangle, northeast Alaska: U.S. Geological Survey Open-File Report 73–310, scale 1:250,000.

_______1973g, Aeromagnetic survey, western half of the Livengood quadrangle, northeast Alaska: U.S. Geological Survey Open-File Report 73–311, scale 1:250,000.

_______1974a, Aeromagnetic map of the Circle quadrangle, northeastern Alaska: U.S. Geological Survey Open-File Report 74–1101, scale 1:250,000.

_______1974b, Aeromagnetic map of eastern half of the Beaver quadrangle, northeastern Alaska: U.S. Geological Survey Open-File Report 74–1102, scale 1:250,000.

_______1974c, Aeromagnetic map of eastern half of the Chandalar quadrangle, northeastern Alaska: U.S. Geological Survey Open-File Report 74–1103, scale 1:250,000.

_______1974d, Aeromagnetic map of eastern half of the Livengood quadrangle, northeastern Alaska: U.S. Geological Survey Open-File Report 74–1104, scale 1:250,000.

Webring, Michael, 1981, MINC—A gridding program based on minimum curvature: U.S. Geological Survey Open-File Report 81–1224, 12 p.

INTERIOR—GEOLOGICAL SURVEY, RESTON, VA—1991

Manuscript approved for publication, August 17, 1988

AEROMAGNETIC MAP OF ALASKA FROM LATITUDE 65°–68° N., LONGITUDE 141°–162° W.: COLOR-SHADED RELIEF

By
John W. Cady
1991

For sale by the U.S. Geological Survey, Map Distribution, Box 25286, Federal Center, Denver, CO 80225